Available online at www.sciencedirect.com
ScienceDirect
Computers and Mathematics with Applications 53 (2007) 232–243
An International Journal
computers & mathematics
with applications
www.elsevier.com/locate/camwa

Transportation of neutral solute in deformable, anisotropic, soft tissue

Le Zhang, Andras Z. Szeri*

Department of Mechanical Engineering, University of Delaware, Newark, DE 19716, United States

Received 13 September 2005; accepted 27 February 2006

Abstract

We present a three-dimensional framework for the transport of neutral solute through soft biological tissue, such as the articular cartilage, under different mechanical loading conditions. The tissue is modelled as a mixture of three phases, a hyperelastic, anisotropic solid matrix, an incompressible inviscid fluid and a solute. The formulation accounts for the anisotropic interaction between the solid and the interstitial water and incorporates the interaction between the solute and the solid matrix. Under the proper circumstances, our model simplifies to biphasic theory and classical convection diffusion.

We find that the pressure gradient variation plays an important role in the neutral solute transport when the soft tissue is dynamically loaded, because of the low concentration of solute present in cartilage. A linear function is suggested for the ratio of friction coefficient between the solute and solid to the friction coefficient between the interstitial water and solid matrix. After validating our model with the experiments of Quinn et al. [T.M. Quinn, C. Studer, A.J. Grodzinsky, J.J. Meister, Preservation and analysis of nonequilibrium solute concentration distributions within mechanically compressed cartilage explants, J. Biochem. Biophys. Methods 52 (2) (2002) 83–95], a numerical study of different dynamic loading conditions on solute transport is carried out.

Keywords: Cartilage; Convection; Diffusion; Deformation; Anisotropic

1. Introduction

Articular cartilage is a specialized soft tissue that covers the ends of articulating bones, making smooth relative motion of the load-bearing surfaces of the diarthrodial joint possible. It also aids the joint in absorbing mechanical shock and, while deforming, it distributes joint load more evenly. Cartilage consists mostly of interstitial water and a solid matrix, the latter is composed of collagen fibre and proteoglycan. The water content of the cartilage is in the range of 65%–80% by net weight.

The distribution of collagen fibres and water is stratified from the surface of the cartilage towards the subchondral bone. The fibres are densely packed and are orientated parallel to the surface of the cartilage within the superficial zone; this zone also has lower proteoglycan content and lower permeability to fluid flow than does the middle zone.

* Corresponding author. Tel.: +1 302 831 2008.
E-mail address: szeri@me.udel.edu (A.Z. Szeri).

0898-1221/$ - see front matter © 2007 Elsevier Ltd. All rights reserved.
doi:10.1016/j.camwa.2006.02.022

There are fewer collagen fibres in the middle zone of the cartilage and these sparser fibres are randomly orientated. The proteoglycan content in the middle zone is relatively large, about 10%–25% by weight. In contrast, in the deep zone the proteoglycan content is lower than in the middle zone and the collagen fibres are orientated perpendicular to the calcified interface. This inhomogeneous and anisotropic structure of the cartilage naturally leads to inhomogeneous and anisotropic transport of the solute. In this paper, however, we do not address inhomogeneity directly.

Leddy and Guilak [2] measured the diffusion coefficient of different size dextrans through the thickness of the cartilage and found it to be site and size specific. For the 3 kDa and the 500 kDa solute, the diffusion coefficients were higher in the surface zone than in the middle and deep zones. In contrast, for the 40 kDa and the 70 kDa solutes the diffusion coefficients were significantly lower in the surface zone than in the middle and deep zones. Leddy and Guilak [3] also noted that diffusion was more rapid in the direction parallel to the collagen fibres than across, and tissue anisotropy had more pronounced effect for the higher molecular weight solute. That is, the ratio D_H/D_V is much larger for large molecules than for small molecules. Here D_H and D_V represent one-dimensional diffusion coefficient parallel with and perpendicular to the articulating surface.

In previous studies, Mauck et al. [4] applied incompressible mixture theory to study neutral solute convective transport under dynamic loading, and examined the diffusion phenomena over a range of the governing non-dimensional parameters. By using a finite element poroelastic model, Ferguson and co-workers [5] studied convective mass transport of solutes in intervertebral disc under the effect of load-induced interstitial flow. Sengers et al. [6] proposed a finite element approach with a biphasic displacement–velocity–pressure description to study solute transport and biosynthesis in soft tissue under dynamic loading. Dispersion due to a non-uniform velocity distribution was incorporated in the model. In these investigations, the formulation assumed isotropic and homogeneous tissue or tissue engineered constructs and the solute transport was considered isotropic and homogeneous.

In an earlier paper [7], we investigated the influence that matrix structure, size of diffusing molecules and the type and intensity of mechanical loading have on the transport of neutral solutes in isotropic tissue, and performed computations under negligible solid–solute interaction. This last restriction prevented us from obtaining good agreement with Quinn's experimental data [1] under conditions of dynamic loading. In the present computations, we do include solid–solute interaction and as a result obtain good agreement with experiments performed under dynamic loading conditions. We then employ our model to investigate the influence of frequency and amplitude of dynamic loading and the influence of static deformation. We also generalize our earlier formulation to provide for tissue anisotropy.

2. Conservation equations

We envisage the soft tissue as consisting of three intrinsically incompressible phases: an inviscid fluid (superscript w, representing the interstitial water), a hyperelastic solid matrix (superscript s, representing the extracellular matrix), and a neutral solute phase (superscript f, representing the nutrients to be transported across the articular surface). It is assumed, therefore, that the mathematical behaviour of the tissue can be characterized by the conservation equations of mixture theory [8–11].

2.1. Conservation of mass

As interconversion of mass among the components is not permitted, the α component mass conservation equation reads

$$\frac{\partial \rho^\alpha}{\partial t} + \operatorname{div}(\rho^\alpha \mathbf{v}^\alpha) = 0, \quad \alpha = s, w, f. \tag{2.1}$$

Alternatively, when taking into account the intrinsic incompressibility of the components of the mixture, we have

$$\frac{\partial \phi^\alpha}{\partial t} + \operatorname{div}(\phi^\alpha \mathbf{v}^\alpha) = 0, \quad \alpha = s, w, f. \tag{2.2}$$

For our saturated mixture $\sum_\alpha \phi^\alpha = 1$, thus summation of Eq. (2.2) over α yields the mixture mass conservation equation

$$\operatorname{div}(\phi^s \mathbf{v}^s + \phi^w \mathbf{v}^w + \phi^f \mathbf{v}^f) = 0. \tag{2.3}$$

2.2. Conservation of linear momentum

For negligible inertia and body force, the mixture momentum equation is

$$\operatorname{div}\mathbf{T} = 0. \tag{2.4}$$

The mixture Cauchy stress $\mathbf{T}$ is the sum of the fluid stress $\mathbf{T}^w$, the matrix stress $\mathbf{T}^s$, and the solute stress $\mathbf{T}^f$

$$\mathbf{T} = \mathbf{T}^s + \mathbf{T}^w + \mathbf{T}^f. \tag{2.5}$$

We postulate the following stress constitutive equations for the solid matrix and the interstitial fluid:

$$\mathbf{T}^s = -\phi^s p\mathbf{I} + 2\rho^s \mathbf{F}\frac{\partial W}{\partial \mathbf{C}}\mathbf{F}^T \tag{2.6}$$

and

$$\mathbf{T}^w = -\phi^w p\,\mathbf{I}. \tag{2.7}$$

If we now disregard $\mathbf{T}^f$ on the assumption of negligible solute volume fraction, Eqs. (2.1)–(2.4) yield the mixture momentum equation

$$\operatorname{div}\left(-p\mathbf{I} + 2\rho^s \mathbf{F}\frac{\partial W}{\partial \mathbf{C}}\mathbf{F}^T\right) = 0. \tag{2.8}$$

In the above equations ρ^s is the density of the solid, $\mathbf{F}$ is the deformation gradient tensor, W is the strain–energy function (for various isotropies, see [12]). $\mathbf{C} = \mathbf{F}^T\mathbf{F}$ is the right Cauchy–Green deformation tensor for the solid, ϕ^s and ϕ^w is the volume fraction of solid matrix and interstitial fluid, and p is the fluid pressure.

For infinitesimal deformation, Eq. (2.8) reduces to

$$\operatorname{div}\left[-p\mathbf{I} + \lambda_s \operatorname{tr}(\mathbf{e})\mathbf{I} + 2\mu_s\mathbf{e}\right] = 0 \tag{2.9}$$

where $\mathbf{e}$ is the infinitesimal strain tensor and λ_s and μ_s are Lame's coefficients. Eq. (2.9) is the first governing equation of the biphasic theory [10].

The momentum equations for the interstitial water and for the neutral solute are:

$$-\rho^w \operatorname{grad}\mu^w + \mathbf{\Pi}_{ws}(\mathbf{v}^s - \mathbf{v}^w) + \pi_{wf}(\mathbf{v}^f - \mathbf{v}^w) = 0 \tag{2.10}$$

$$-\rho^f \operatorname{grad}\mu^f + \pi_{fs}(\mathbf{v}^s - \mathbf{v}^f) + \pi_{wf}(\mathbf{v}^w - \mathbf{v}^f) = 0. \tag{2.11}$$

Here ρ^α represent the density, μ^α the chemical potential, and $\mathbf{v}^\alpha$ the velocity for the α component. Inertia and viscous effects have been neglected when writing Eqs. (2.10) and (2.11).

It follows from the entropy production inequality that $\mathbf{\Pi}_{ws}$, the drag coefficient characterizing matrix–fluid interaction, is a positive definite second-order tensor [13]; if the pore structure of the tissue is isotropic than $\mathbf{\Pi}_{ws} = \pi_{ws}\mathbf{I}$ is a scalar multiple of the unit tensor, for anisotropic matrix it is a general tensor. We assume, however, that particle–solid and particle–fluid interactions can be adequately modelled by the scalar coefficients π_{sf} and π_{wf}.

Constitutive equations for the chemical potentials μ^w, μ^f are those of Mauck et al. [4]

$$\mu^w = \mu_0^w(\theta) + \frac{1}{\rho_T^w}(p - R\theta\Phi c^f) \tag{2.12}$$

$$\mu^f = \mu_0^f(\theta) + \frac{R\theta}{M_f}\ln(\gamma^f c^f) \tag{2.13}$$

where the μ_0^α, $\alpha = w, f$, are the reference potentials for water and solute, R is the universal gas constant, θ is the absolute temperature of the mixture, Φ is the osmotic coefficient, c^f is the molar concentration of the solute, γ_f is the mean activity coefficient, ρ_T^f is the true density for the solute and $\rho^f = \phi^w c^f M_f$ is its apparent density. This last relation follows from the definitions

$$\rho^\alpha = \frac{\mathrm{d}m^\alpha}{\mathrm{d}V}, \qquad \phi^\alpha = \frac{\mathrm{d}V^\alpha}{\mathrm{d}V}, \qquad \rho_T^\alpha = \frac{\mathrm{d}m^\alpha}{\mathrm{d}V^\alpha}, \qquad c^\alpha = \frac{\mathrm{d}n^\alpha}{\mathrm{d}V^w}, \qquad M_\alpha = \frac{\mathrm{d}m^\alpha}{\mathrm{d}n^\alpha}. \tag{2.14}$$

Here V is the mixture volume and V^α, m^α, M_α, and n^α represents the volume, the mass, the mole number, and the number of molecules of the α component. As we have no further interest in c^α and M_α for $\alpha = s, w$, we set $c \equiv c^f$, $\gamma \equiv \gamma_f$ and $M \equiv M_f$ in the sequel.

3. Derivation of the governing equations

Assuming that the solute volume fraction is negligible, $\phi^f \ll 1$, we find the velocity of the solid phase from the approximation to Eq. (2.3) as

$$\operatorname{div} \mathbf{v}^s + \operatorname{div}[\phi^w(\mathbf{v}^w - \mathbf{v}^s)] = 0. \tag{3.1}$$

The volume fractions ϕ^s and ϕ^w are now related through $\phi^s \approx 1 - \phi^w$ for saturated medium; we put $\phi = \phi^w$ and employ only ϕ throughout the sequel.

3.1. The momentum equations

Eq. (2.11) is now recast into

$$-\rho^f \operatorname{grad} \mu^f + \pi_{fs}(\mathbf{v}^s - \mathbf{v}^w) + (\pi_{fs} + \pi_{wf})(\mathbf{v}^w - \mathbf{v}^f) = 0. \tag{3.2}$$

Combining Eqs. (3.2) and (2.10), we obtain the relative velocity between interstitial water and solute as

$$\mathbf{v}^f - \mathbf{v}^w = \mathbf{\Omega}[\rho^w \pi_{fs} \operatorname{grad} \mu^w - \rho^f \mathbf{\Pi}_{ws} \operatorname{grad} \mu^f]. \tag{3.3}$$

For expediency, we employ the notation $\mathbf{\Omega} = (\pi_{wf}\pi_{fs}\mathbf{I} + \pi_{fs}\mathbf{\Pi}_{ws} + \pi_{wf}\mathbf{\Pi}_{ws})^{-1}$ and introduce expression (3.3) into the momentum equation for the water phase, Eq. (2.10) to obtain

$$\mathbf{v}^s - \mathbf{v}^w = \rho^w \mathbf{\Pi}_{ws}^{-1} \operatorname{grad} \mu^w - \pi_{wf} \mathbf{\Pi}_{ws}^{-1} \mathbf{\Omega}[\rho^w \pi_{fs} \operatorname{grad} \mu^w - \rho^f \mathbf{\Pi}_{ws} \operatorname{grad} \mu^f]. \tag{3.4}$$

Substitution of Eqs. (2.12) and (2.13) for chemical potentials into Eq. (3.4) yields

$$\begin{aligned} &\mathbf{v}^s - \mathbf{v}^w \\ &= \left\{ \phi \left[\mathbf{\Pi}_{ws}^{-1} \left(\mathbf{I} - \pi_{fs}\pi_{wf}\mathbf{\Omega} \right) \operatorname{grad} p - R\theta\, \mathbf{\Pi}_{ws}^{-1} \left((\mathbf{I} - \pi_{fs}\pi_{wf}\mathbf{\Omega}) \operatorname{grad}(\Phi c) - \frac{\pi_{wf}}{\gamma} \mathbf{\Omega}\mathbf{\Pi}_{ws} \operatorname{grad}(\gamma c) \right) \right] \right\}. \end{aligned} \tag{3.5}$$

On recasting Eq. (3.5) into the form

$$\phi(\mathbf{v}^s - \mathbf{v}^w) = \left\{ \mathbf{K} \operatorname{grad} p - R\theta \left[\mathbf{K} \operatorname{grad}(\Phi c) - \frac{\phi^2 \pi_{wf}}{\gamma} \mathbf{\Pi}_{ws}^{-1} \mathbf{\Omega}\mathbf{\Pi}_{ws} \operatorname{grad}(\gamma c) \right] \right\} \tag{3.6}$$

we easily recognize it as a generalization of Darcy's law, where

$$\mathbf{K} = \phi^2 \mathbf{\Pi}_{ws}^{-1} (\mathbf{I} - \pi_{wf}\pi_{fs}\mathbf{\Omega}) \tag{3.7}$$

is designated the permeability tensor.

For $\gamma = \Phi = 1$, and assuming that $\pi_{fs} = 0$, we obtain the second governing equation of the biphasic theory [14].

$$\phi(\mathbf{v}^w - \mathbf{v}^s) = -\mathbf{K} \operatorname{grad} p, \quad \mathbf{K} = \phi^2 \mathbf{\Pi}_{ws}^{-1}. \tag{3.8}$$

By eliminating the relative velocity $(\mathbf{v}^w - \mathbf{v}^s)$ between Eqs. (3.1) and (3.6), we further obtain an expression for the velocity of the solid matrix

$$\operatorname{div} \mathbf{v}^s - \operatorname{div} \left[\mathbf{K} \operatorname{grad}(p - R\theta\, \Phi c) + \frac{R\theta\phi^2\pi_{wf}}{\gamma} \mathbf{\Pi}_{ws}^{-1} \mathbf{\Omega}\mathbf{\Pi}_{ws} \operatorname{grad}(\gamma c) \right] = 0. \tag{3.9}$$

3.2. The convection/diffusion equation

By substituting for the solute velocity from Eq. (3.3) into Eq. (2.1) for the solute we obtain

$$\frac{\partial \rho^f}{\partial t} - \operatorname{div}[\rho^f \mathbf{\Omega}(\rho^f \mathbf{\Pi}_{ws} \operatorname{grad} \mu^f - \rho^w \pi_{fs} \operatorname{grad} \mu^w) - \rho^f \mathbf{v}^w] = 0. \tag{3.10}$$

Substituting the constitutive Eqs. (2.12) and (2.13) into Eq. (3.10), and utilizing the formula $\rho^f = \phi c M$, we derive the convection/diffusion equation in anisotropic porous material

$$\frac{\partial c}{\partial t} + \mathbf{v}^w \cdot \operatorname{grad} c - \frac{1}{\phi} \operatorname{div} \left\{ \phi^2 c \mathbf{\Omega} \left[R\theta \left(\frac{1}{\gamma} \mathbf{\Pi}_{ws} \operatorname{grad}(\gamma c) + \pi_{fs} \operatorname{grad}(\Phi c) \right) - \pi_{fs} \operatorname{grad} p \right] \right\} = 0. \tag{3.11}$$

If, in analogy with Zhang and Szeri [7], we now define the diffusion coefficient tensor

$$\mathbf{D} = R\theta c \phi^2 \mathbf{\Omega} \mathbf{\Pi}_{ws}. \tag{3.12}$$

Eq. (3.11) then takes the form

$$\frac{\partial c}{\partial t} + \mathbf{v}^w \cdot \operatorname{grad} c - \frac{1}{\phi} \operatorname{div} \left\{ \mathbf{D} \left[\frac{1}{\gamma} \operatorname{grad}(\gamma c) + \pi_{fs} \mathbf{\Pi}_{ws}^{-1} \operatorname{grad}(\Phi c) \right] - \phi^2 c \pi_{fs} \mathbf{\Omega} \operatorname{grad} p \right\} = 0. \tag{3.13}$$

On setting $\gamma = 1, \pi_{fs} = 0$ in Eq. (3.13), we recover the classical form of the convection diffusion equation for nonisotropic porous medium [15]

$$\phi \frac{\partial c}{\partial t} + \phi \mathbf{v}^w \cdot \operatorname{grad} c - \operatorname{div}[\mathbf{D} \operatorname{grad} c] = 0. \tag{3.14}$$

In summary, our model for neutral particle diffusion in a cartilage undergoing large deformation is defined by the following system of coupled, nonlinear equations

$$\operatorname{div} \left(-p\mathbf{I} + 2\rho^s \mathbf{F} \frac{\partial W}{\partial \mathbf{C}} \mathbf{F}^T \right) = 0 \tag{3.15}$$

$$\operatorname{div} \mathbf{v}^s - \operatorname{div} \left\{ \mathbf{K} \operatorname{grad} p - R\theta \left[\mathbf{K} \operatorname{grad}(\Phi c) - \frac{\phi^2 \pi_{wf}}{\gamma} \mathbf{\Pi}_{ws}^{-1} \mathbf{\Omega} \mathbf{\Pi}_{ws} \operatorname{grad}(\gamma c) \right] \right\} = 0 \tag{3.16a}$$

$$\mathbf{v}^w = \mathbf{v}^s - \frac{1}{\phi} \left\{ \mathbf{K} \operatorname{grad} p - R\theta \left[\mathbf{K} \operatorname{grad}(\Phi c) - \frac{\phi^2 \pi_{wf}}{\gamma} \mathbf{\Pi}_{ws}^{-1} \mathbf{\Omega} \mathbf{\Pi}_{ws} \operatorname{grad}(\gamma c) \right] \right\} \tag{3.17a}$$

$$\frac{\partial c}{\partial t} + \mathbf{v}^w \cdot \operatorname{grad} c - \frac{1}{\phi} \operatorname{div} \left\{ \mathbf{D} \left[\frac{1}{\gamma} \operatorname{grad}(\gamma c) + \pi_{fs} \mathbf{\Pi}_{ws}^{-1} \operatorname{grad}(\Phi c) \right] - \phi^2 c \pi_{fs} \mathbf{\Omega} \operatorname{grad} p \right\} = 0. \tag{3.18a}$$

Eqs. (3.16a)–(3.18a) take different form depending on our assumptions on material properties:

(a) For $\Phi = 1$ and $\gamma = 1$:

$$\operatorname{div} \mathbf{v}^s - \operatorname{div}[\mathbf{K} \operatorname{grad} p - R\theta(\mathbf{K} - \phi^2 \pi_{wf} \mathbf{\Pi}_{ws}^{-1} \mathbf{\Omega} \mathbf{\Pi}_{ws}) \operatorname{grad} c] = 0 \tag{3.16b}$$

$$\mathbf{v}^w = \mathbf{v}^s - \frac{1}{\phi} [\mathbf{K} \operatorname{grad} p - R\theta(\mathbf{K} - \phi^2 \pi_{wf} \mathbf{\Pi}_{ws}^{-1} \mathbf{\Omega} \mathbf{\Pi}_{ws}) \operatorname{grad} c] \tag{3.17b}$$

$$\frac{\partial c}{\partial t} + \mathbf{v}^w \cdot \operatorname{grad} c - \frac{1}{\phi} \operatorname{div}[\mathbf{D}(\mathbf{I} + \pi_{fs} \mathbf{\Pi}_{ws}^{-1}) \operatorname{grad} c - \phi^2 c \pi_{fs} \mathbf{\Omega} \operatorname{grad} p] = 0. \tag{3.18b}$$

(b) For isotropic tissue we put $\omega = 1/(\pi_{wf}\pi_{fs} + \pi_{fs}\pi_{ws} + \pi_{wf}\pi_{ws})$ so that $\mathbf{\Omega} = \omega \mathbf{I}$ and derive the simplified equations

$$\operatorname{div} \mathbf{v}^s - \operatorname{div} \left\{ k \left[\operatorname{grad} p + R\theta \left(\frac{\pi_{wf}}{\gamma(\pi_{fs} + \pi_{wf})} \operatorname{grad}(\gamma c) - \operatorname{grad}(\Phi c) \right) \right] \right\} = 0 \tag{3.16c}$$

$$\mathbf{v}^w = \mathbf{v}^s - \frac{k}{\phi}\left\{\text{grad}\, p + R\theta\left[\frac{\pi_{wf}}{\gamma(\pi_{fs}+\pi_{wf})}\text{grad}(\gamma c) - \text{grad}(\Phi c)\right]\right\} \tag{3.17c}$$

$$\frac{\partial c}{\partial t} + \mathbf{v}^w \cdot \text{grad}\, c - \frac{1}{\phi}\text{div}\left\{D\left[\frac{1}{\gamma}\text{grad}(\gamma c) + \frac{\pi_{fs}}{\pi_{ws}}\text{grad}(\Phi c)\right] - \phi^2 c\pi_{fs}\omega\text{grad}\, p\right\} = 0. \tag{3.18c}$$

In this case the permeability k, now a scalar, changes with porosity, and indirectly with strain, according to

$$k = k_0 \exp\left[M\left(\frac{\phi-\phi_0}{1-\phi}\right)\right]. \tag{3.19}$$

Eq. (3.19) derived from one-dimensional experiments by Lai and Mow [16]. Here ϕ_0 is the volume fraction of the interstitial fluid in the undeformed matrix at zero load; in finite deformation it is related to ϕ through [7]

$$\phi = 1 - (1-\phi_0)\det \mathbf{C}^{-1/2}. \tag{3.20}$$

For infinitesimal strain $\det \mathbf{C}^{1/2} = 1 + \text{tr}\,\mathbf{e}$.

The diffusion coefficient D is related to porosity according to Yasuda et al. [7,17]

$$\frac{D}{D_0} = \exp\left[K\left(\frac{\phi-\phi_0}{\phi\phi_0}\right)\right]. \tag{3.21}$$

4. Computational issues

For ease of computations and due to lack of more general experimental data, our numerical work assumes $\gamma = \Phi = 1$ and postulates infinitesimal deformation of the soft tissue. In that case then the governing equations for solute transport in isotropic soft tissue reduce to

$$\text{div}[-p\mathbf{I} + \lambda_s \text{tr}(\mathbf{e})\mathbf{I} + 2\mu_s\mathbf{e}] = 0 \tag{4.1}$$

$$\text{div}\,\mathbf{v}^s - \text{div}\left\{k\left[\text{grad}\, p - R\theta\left(\frac{\pi_{fs}}{\pi_{fs}+\pi_{wf}}\right)\text{grad}\, c\right]\right\} = 0 \tag{4.2}$$

$$\mathbf{v}^w = \mathbf{v}^s - \frac{k}{\phi}\left[\text{grad}\, p - R\theta\left(\frac{\pi_{fs}}{\pi_{fs}+\pi_{wf}}\right)\text{grad}\, c\right] \tag{4.3}$$

$$\frac{\partial c}{\partial t} + \mathbf{v}^w \cdot \text{grad}\, c - \frac{1}{\phi}\text{div}\left\{D\left(\frac{\pi_{ws}+\pi_{fs}}{\pi_{ws}}\right)\text{grad}\, c - \frac{D}{R\theta}\left(\frac{\pi_{fs}}{\pi_{ws}}\right)\text{grad}\, p\right\} = 0 \tag{4.4}$$

$$\begin{aligned}
&\phi = 1 - (1-\phi_0)/(1+\text{tr}\,\mathbf{e})\\
&k = k_0 \exp\left[M\left(\frac{\phi-\phi_0}{1-\phi}\right)\right]\\
&D = D_0 \exp\left[K\left(\frac{\phi-\phi_0}{\phi\phi_0}\right)\right].
\end{aligned} \tag{4.5}$$

Eq. (4.3) clarifies that two fields are responsible for the flow of interstitial water, the pressure field of the external load and the concentration field of the solute. Of these, the pressure field has the controlling influence. In support of this statement we refer to Ferguson [5] "as in vivo concentration of neutral solutes such as glucose, enzymes and cytokines are several orders of magnitude lower than the concentration of ions, the presence of such solute has no influence on the fluid transport". The work of Urban et al. [18] leads to the same conclusion; the magnitude of neutral solute concentration varies from 10^{-3} to 10^{-7} M, while, for normal physiological loading, the magnitude of pore pressure is of order 10^6 Pa and the ratio $R\theta c/p$ is of order 10^{-3}–10^{-7}. Since $0 \le \pi_{fs}/(\pi_{fs}+\pi_{wf}) \le 1$,

$$\left(\frac{\pi_{fs}}{\pi_{fs}+\pi_{wf}}\right) R\theta c \ll p$$

and may be neglected in computation.

It is now our intension to estimate the order of magnitude of π_{fs}/π_{ws} of Eq. (4.4) from experimental data adopted from the literature. Lai and Mow [16] and Lai et al. [19] reported that $\pi_{ws} \approx (10^{15}$–$10^{16})$ in N s/m^4. Mauck et al. [4] listed diffusion coefficients in cartilage, $D \approx 10^{-11}$–10^{-12} m^2/s, and in pure water, $D^{wf} \approx 10^{-11}$ m^2/s, as well as the correlation between friction coefficient and the diffusion coefficient, viz., $D = \phi R\theta c/(\pi_{wf} + \pi_{sf})$ and $D^{wf} = \phi R\theta c/\pi_{wf}$. Substitution of representative values for R, θ and c, we find that $\pi_{fs}/\pi_{ws} = O(10^{-5}$–$10^{-4})$ for neutral solutes with about 10^{-6} M concentration.

Next, we indicate that the ratio of the friction coefficients π_{sf}/π_{ws} is not a constant. For this, we sum Eqs. (2.10) and (2.11), the momentum equations for water and solute, and substitute for the chemical potentials from Eqs. (2.12) and (2.13), to arrive at

$$-\phi^w \text{grad}(p - R\theta c) - \phi^w R\theta \text{grad}\, c + \mathbf{\Pi}_{ws}(\mathbf{v}^s - \mathbf{v}^w) + \pi_{fs}(\mathbf{v}^s - \mathbf{v}^f) = 0. \tag{4.6}$$

Setting $\gamma = \Phi = 1$, for isotropic tissue Eq. (4.6) simplifies to

$$\pi_{ws}(\mathbf{v}^s - \mathbf{v}^w) + \pi_{fs}(\mathbf{v}^s - \mathbf{v}^f) = \phi^w \text{grad}\, p. \tag{4.7}$$

Taking the divergence of Eq. (4.7) yields

$$\pi_{ws}\text{div}\,(\mathbf{v}^s - \mathbf{v}^w) + \pi_{fs}\text{div}(\mathbf{v}^s - \mathbf{v}^f) = \phi^w \nabla^2 p \tag{4.8}$$

and

$$\frac{\pi_{fs}}{\pi_{ws}} = \frac{\pi_{ws}^{-1}\phi^w \nabla^2 p - \text{div}\,(\mathbf{v}^s - \mathbf{v}^w)}{\text{div}\,(\mathbf{v}^s - \mathbf{v}^f)}. \tag{4.9}$$

Eq. (4.9) indicates that the ratio π_{sf}/π_{ws} varies as the Laplacien of the pressure. However, as we were unable to find soft tissue data on this influence of pressure, we assume linear dependence according to

$$\frac{\pi_{fs}}{\pi_{ws}} = a_0 + a_1 \frac{r_0^2 k_0}{D_0}\nabla^2 p \tag{4.10}$$

where a_0 and a_1 are material constants (presently, we fix the magnitude of a_0 at 10^{-5}–$10^{-4)}$.

Obviously, Eq. (4.10) cannot be viewed as a constitutive equation for the ratio π_{sf}/π_{ws}; experimental investigation is needed to determine the exact expression. Spielger [20] proposed to derive the friction coefficients from measurements of phenomenological coefficients of the mixture.

We implement our model, consisting of Eqs. (4.1)–(4.5), in the commercial finite element code ABAQUS. The numerical solution of the equations is performed in two steps. First we solve Eqs. (4.1) and (4.2), employing solid consolidation procedure. Second, we solve Eq. (4.4) using the heat transfer procedure in ABAQUS, treating the term

$$\frac{1}{\phi}\,\text{div}\left[\frac{D}{R\theta}\left(\frac{\pi_{fs}}{\pi_{ws}}\right)\text{grad}\, p\right]$$

as the heat source.

5. Model validation

To demonstrate the viability of our model, we compare its theoretical predictions with the experimental data of Quinn et al. [1]. Quinn and co-workers reported on a fluorescence-based method for the observation of solute concentration during desorption in statically and dynamically compressed cartilage explants.

Quinn's experiments were performed on 0.65 mm thick and 2.7 mm diameter cartilage disks, harvested from 18-months old cows. Prior to the experiments, the disks were soaked in a PBS (phosphate buffered saline) bath containing either 3 kDa at 0.75 μM or 40 kDa at 1.5 μM dextrans, conjugated to TMR (tetramethylrhodamine, a fluorescent). After equilibration, the samples were immersed in another PBS bath, large in volume and well agitated to assure zero concentration boundary condition at sample radial edges, and compressed axially, without radial confinement, between impermeable platens. Laser confocal measurements of fluorescence intensity were made, after allowing for 1 h of radial solute desorption under the prescribed loading. Unfortunately, the paper does not list the values of some of the parameters pertinent to the experiments; these needed to be assumed [7], and are listed in Table 1.

Table 1
Material parameters (assumed) for Quinn's experimental data

	3 kDa dextran	40 kDa dextran
Initial diffusion coeff., D_0	31 $\mu m^2/s$	40 $\mu m^2/s$
Young's modulus, E	0.6 MPa	0.8 MPa
Poisson's ratio, μ	0.165	0.12
Permeability, k_0	1.2e–15 m^4/N s	8.5e–15 m^4/N s
Size coefficient, K	6.65	12.8
Porosity, ϕ_0^w	0.78	0.8
Permeability exp., M	4.2	8.1
a_0	1.0e–4	
a_1	5.27e–6	

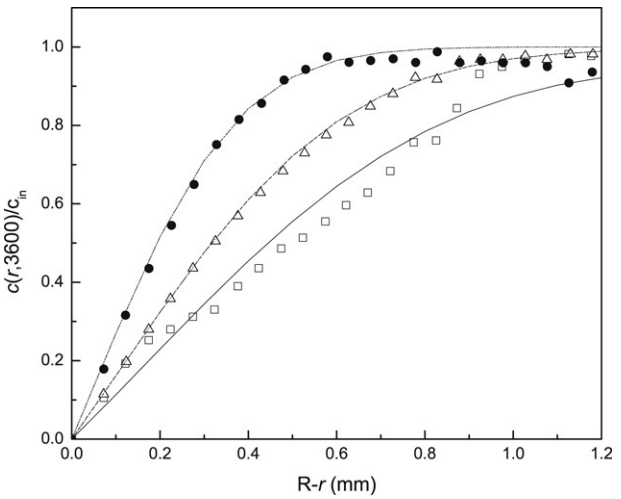

Fig. 1a. Concentration distribution of 40 kDa dextran, static loading: (Symbols: Quinn et al., 2002; Cuves: theory; □, — current model, —·— $\pi_{fs} = 0$, $\varepsilon = 10\%$; △, – – current model, –·–·– $\pi_{fs} = 0$, $\varepsilon = 15\%$; ●, · · · · · current model, – – – $\pi_{fs} = 0$, $\varepsilon = 31\%$).

5.1. Static loading

The pressure distribution becomes uniform as the tissue reaches its equilibrium state under static loading; therefore, the effect of the pressure gradient source term in Eq. (4.4) vanishes. In the static load experiments of Quinn et al. [1], the tissue was allowed to stress-relax long enough prior to the experiment to minimize the effects of compression-induced convection. Hence, in accordance with Eq. (3.12), under static loading conditions solute–solid interaction can influence solute transport only through the diffusion coefficient; this effect is shown to be negligible in Fig.1. Here we recomputed Quinn's static data; our new results are hardly distinguishable from those in [7], which neglected the interaction between the solute and solid.

5.2. Dynamic loading

The dynamic loading condition in Quinn's experiments was 23% offset static strain plus 5% dynamic strain. Fig. 2 shows the normalized desorption concentration $\bar{c} = c(r, 3600)/c_{\text{in}}$ versus radial distance $R - r$, obtained with initial value $c(r, 0) = c_{\text{in}}, r < R$. The symbols in Fig. 2 correspond to Quinn's experimental data at the frequency of $f = 0.001$. The continuous curve is the predictions of the current model. Agreement is satisfactory when the pressure source term of Eq. (4.4) is included in the computations; this is not the case when the pressure term is omitted (dashed curve, from [7]). Here we attribute the falling off of the data for $R - r > 1.0$ to systematic experimental error.

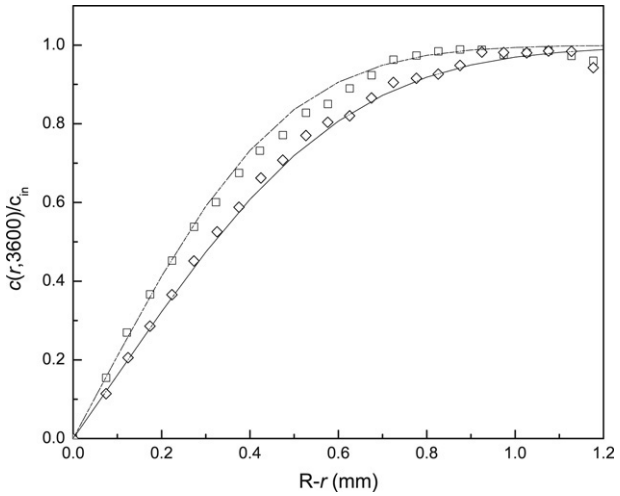

Fig. 1b. Concentration distribution of 3 kDa dextran, static loading. (Symbols: Quinn et al., 2002; Cuves: theory; □, — current model, —·— $\pi_{fs} = 0$, $\varepsilon = 15\%$; Δ, – – current model, –···– $\pi_{fs} = 0$, $\varepsilon = 31\%$).

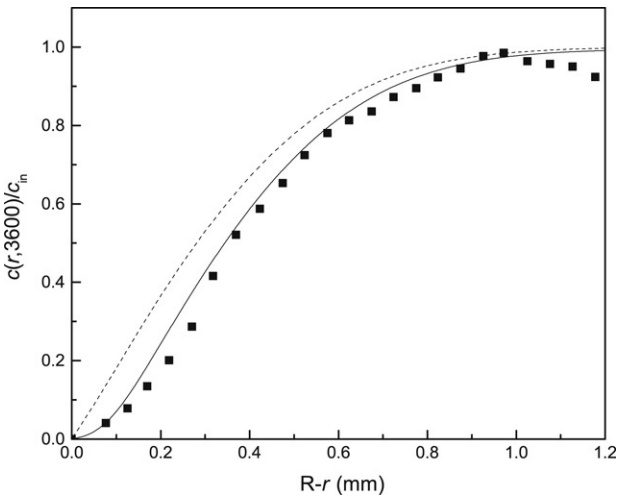

Fig. 2. Concentration distribution of 3 kDa dextran, dynamic loading (23% static compression + 5% dynamic compression). (□ Quinn et al., 2002; —, current model, – – $\pi_{fs} = 0$).

6. Results and conclusions

We intend to apply our model, Eqs. (4.1)–(4.5) and (4.10), to investigate the effect of the loading conditions, i.e. variation of frequency, amplitude of the dynamic loading and the offset static loading, on the transport of solutes in articular cartilage. The parameters are held fixed during the computations. Suspecting that some of the fitted parameters of the model might be frequency dependent (e.g. the coefficients a_0 and a_1 in the equation for π_{sf}/π_{ws}) we restrict our study of solute transport to a small neighbourhood of the parameters of Quinn's experiments and indicate only directions of change of performance as input parameters are varied.

6.1. Effect of frequency of dynamic load

Fig. 3 shows the variation of concentration distribution, corresponding to a variation of the frequency of dynamic loading. The amplitude of dynamic strain was kept at 5% and the offset static strain at 23% during these computations. Solute concentration is higher when the tissue experiences static loading only, in contrast to when it is loaded

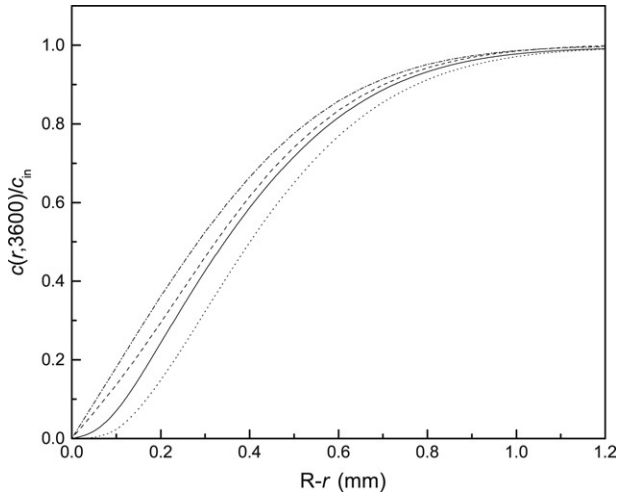

Fig. 3. Concentration distribution of 3 kDa dextran under dynamic loading with various frequencies. (— · — $f = 0.0$, – – $f = 0.0005$, — $f = 0.001$, – – – $f = 0.002$).

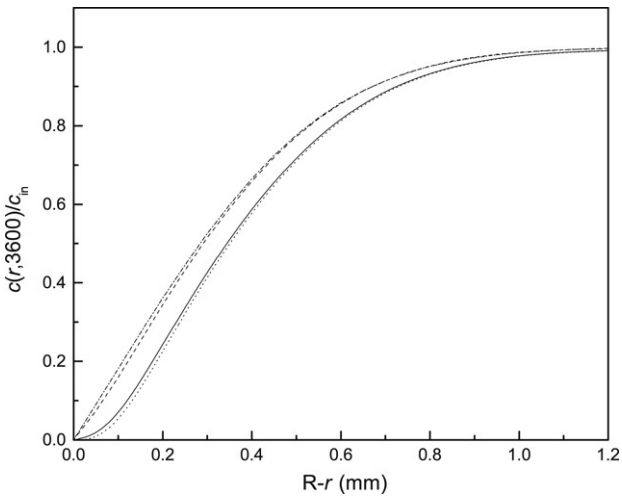

Fig. 4. Concentration distribution of 3 kDa dextran under dynamic loading with various amplitude. (— · — $a = 0.0\%$, – – $a = 2.0\%$, — $a = 5.0\%$, – – – $a = 6.0\%$).

dynamically at frequencies between 0.0005 and 0.002 Hz, signifying that solute desorption is facilitated in this frequency range. Fig. 3 also shows that solute transport decreases as the frequency is lowered from 0.001 to 0.0005 Hz. In contrasting to this, solute desorption increases as the frequency is increased from 0.001 to 0.002 Hz.

6.2. *Effect of amplitude of dynamic load*

Fig. 4 illustrates the effect the oscillatory amplitude has on solute desorption. We keep the frequency of dynamic loading at 0.001 Hz and the offset static strain as 23% during these computations. There is little effect on solute transport as the dynamic amplitude is decreased to 0.02, compared to solute transport when the tissue is under static loading only. (Interestingly, Sah et al. [21] pointed out that at frequency from 0.0001–0.001, amplitude up to 4% had negligible effect on ^{3}H-proline and ^{35}S-sulfate incorporation. ^{3}H-proline denoted the glycosaminoglycan synthesis, and ^{35}S-sulfate denoted amino acid uptake and protein synthesis). Fig. 4 also shows that the solute desorption is not affected significantly as we increase the dynamic amplitude from 5% to 6%.

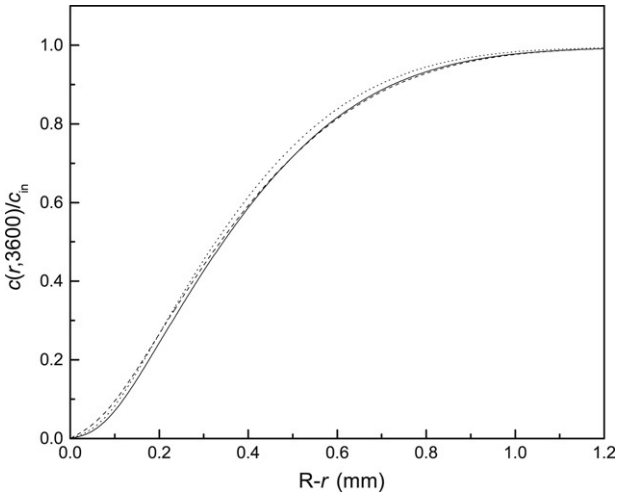

Fig. 5. Concentration distribution of 3 kDa dextran under dynamic loading with various offset static strain. ($--\ \varepsilon = 20\%$; $—\ \varepsilon = 23\%$; $\varepsilon = 25\%$).

6.3. Effect of offset strain

In Fig. 5, we investigate the effect of variation of offset static strain on solute transport. In the computations, we keep the frequency of dynamic loading at 0.001 Hz, and the dynamic strain at 5%. Fig. 5 shows that there is no significant effect of offset static strain on solute transport in cartilage explants as the offset strain varies from 20% to 25%.

6.4. Conclusions

A nonlinear mathematical model for the transport of neutral solutes through soft biological tissue is developed based on mixture theory. The model incorporates the interaction between the solute and solid, identifying the pressure gradient as an additional source term in the diffusion equation. This term is influential for neutral solute transport as the large neutral solute concentration is low in soft tissue. The formulation is capable of simultaneously describing the deformation of anisotropic soft tissue and its nutrient or regulator transport within the tissue. An understanding of these phenomena would provide insights of tissue biosynthesis under physiological environment and help to control the loading condition for the tissue engineered constructs.

Acknowledgement

This publication was made possible by Grant Number P20RR16458 from the National Center for Research Resources (NCRR), a component of the National Institutes of Health (NIH). Its contents are solely the responsibility of the authors and do not necessarily represent the official views of NCRR or NIH.

References

[1] T.M. Quinn, C. Studer, A.J. Grodzinsky, J.J. Meister, Preservation and analysis of nonequilibrium solute concentration distributions within mechanically compressed cartilage explants, J. Biochem. Biophys. Methods 52 (2) (2002) 83–95.
[2] H.A. Leddy, F. Guilak, Site-specific molecular diffusion in articular cartilage measured using fluorescent recovery after photo bleaching, Ann. Biomed. Eng. 31 (2003) 753–760.
[3] H.A. Leddy, F. Guilak, Anisotropic diffusion of macromolecules in articular cartilage, in: 50th Annual meeting of the Orthopaedic Research Society. No. 0229, 2004.
[4] R.L. Mauck, C.T. Hung, G.A. Ateshian, Modeling of neutral solute transport in a dynamically loaded porous permeable gel: Implications for articular cartilage biosynthesis and tissue engineering, J. Biomech. Eng. 125 (2003) 602–614.
[5] S.J. Ferguson, K. Ito, L.P. Nolte, Fluid flow and convective transport of solutes within the intervertebral disc, J. Biomech. 37 (2004) 213–221.
[6] B.G. Sengers, C.W.J. Oomens, F.P.T. Baaijens, An integrated finite-element approach to mechanics, transport and biosynthesis in tissue engineering, J. Biomech. Eng. Trans. ASME 126 (2004) 82–91.

[7] L. Zhang, A.Z. Szeri, Transport of neutral solute in articular cartilage: Effects of loading and particle size, Proc. R. Soc. A 46 (2005) 2021–2042.
[8] R.J. Atkin, R.E. Craine, Continuum theories of mixtures: Basic theory and historical development, Quart. J. Mech. Appl. Math. XXIX (1976) 209–244.
[9] R.M. Bowen, Incompressible porous media models by use of the theory of mixtures, Internat. J. Engrg. Sci. 18 (1980) 1129–1148.
[10] V.C. Mow, S.C. Kuei, W.M. Lai, C.G. Armstrong, Biphasic creep and stress-relaxation of articular-cartilage in compression — theory and experiments, J. Biomech. Eng. Trans. ASME 102 (1) (1980) 73–84.
[11] K.R. Rajagopal, L. Tao, Mechanics of Mixtures, World Scientific Publishing Co., 1995.
[12] A.E. Green, J. Adkins, Large Elastic Deformations, University Press, Oxford, 1970.
[13] L. Tao, J.D. Humphrey, K.R. Rajagopal, A mixture theory for heat-induced alterations in hydration and mechanical properties in soft tissues, Internat. J. Engrg. Sci. 39 (14) (2001) 1535–1556.
[14] E.S. Almeida, R.L. Spilker, Finite element formulations for hyperelastic transversely isotropic biphasic soft tissues, Comput. Methods Appl. Mech. Engrg. 151 (3–4) (1998) 513–538.
[15] D.A. Nield, A. Bejan, Convection in Porous Media, Springer-Verlag, New York, 1992.
[16] W.M. Lai, V.C. Mow, Drag-induced compression of articular cartilage during a permeation experiment, Biorheology 17 (1980) 111–123.
[17] H. Yasuda, C.E. Lamaze, L.D. Ikenberry, Permeability of solutes through hydrated polymer membranes, Makromolekul. Chem. 118 (1968) 19–35.
[18] J.P.G. Urban, S. Simth, J.C.T. Fairbank, Nutrition of the intervertebral disc, Spine 170 (2004) 296–302.
[19] W.M. Lai, V.C. Mow, W.B. Zhu, Constitutive modeling of articular-cartilage and biomacromolecular solutions, J. Biomech. Eng. Trans. ASME 115 (4) (1993) 474–480.
[20] K.S. Spielger, Transport process in inonic membrane, Trans. Faraday Soc. 54 (9) (1958) 1408–1428.
[21] R.L. Sah, Y.J. Kim, J.Y. Doong, A.J. Grodzinsky, A.H. Plaas, J.D. Sandy, Biosynthetic response of cartilage explants to dynamic compression, J. Orthop. Res. 7 (5) (1989) 619–636.